Figure 2. Molecular structure and labeling scheme (50% probability) of (Ind)W(CO)₂PPh₃Cl (2). Selected bond lengths (Å): W–C(1) = 2.279 (6); W–C(2) = 2.291 (7); W–C(3) = 2.469 (6); W–C(8) = 2.476 (7); W–C(9) = 2.307 (6); W–P = 2.516 (1); W–Cl = 2.492 (2); W–C(10) = 1.936 (7); W–C(11) = 1.947 (7). Selected bond angles (deg): P–W–C(11) = 79.9 (2); P–W–Cl = 78.38 (5); C(10)–W–C(11) = 72.5 (3); Cl–W–C(10) = 79.7 (2).

atom has slipped a distance $|S|$ = 0.132 Å away from the centroid along a vector α = 34° relative to the centroid–C(1) axis; the difference between the mean W to C(2), C(1), and C(9) distance and the mean W to C(3) and C(8) distance is $\Delta(\overline{W-C})$ = 0.14 Å, and the dihedral angle between the plane of C(2)–C(1)–C(9) and the best-fit plane of C(2)–C(3)–C(8)–C(9) is Ω = 7.6°. These values differ only slightly from the values of $|S|$ = 0.138 Å, α = 79°, $\Delta(\overline{Mo-C})$ = 0.11 Å, and Ω = 9.6° obtained from the structure of (Ind)Mo(CO)₃I by Mawby and Pringle.[10]

Discussion

Ligand substitution in (Ind)W(CO)₃Cl (1) is orders of magnitude faster than in the parent CpW(CO)₃Cl and occurs by competitive associative and dissociative pathways. Thus, in addition to the expected promotion of the associative mechanism, the indenyl ligand has also enhanced the rate of ligand dissociation in 1. To a lesser extent the same is true of 3.

Ligand substitution is also faster in 1 than in the isostructural Mo compounds (Ind)Mo(CO)₃X (X = Cl, Br, I) studied by Mawby.[2] The difference is largely in the associative pathway. Associative substitution by PPh₃ is approximately 37 times faster in 1 than in (Ind)Mo(CO)₃Cl under comparable conditions, whereas the dissociative pathway is in fact faster in the Mo complex. Some pertinent data are summarized in Table III. This difference is most evident in a comparison of the rate constant ratio k_a/k_d. The ratio k_a/k_d is consistently less than 1.0 for the reaction of the Mo complexes with PPh₃ but large for reaction of 1 with PPh₃ and 3 with P(OPh)₃. Even the most nucleophilic ligand employed by Mawby, PBu₃, only achieved a ratio of k_a/k_d = 15.1.

The associative pathway appears to be more strongly influenced by the steric bulk of the entering ligand than by its electron-donor properties. Associative substitution in both 1 and 3 is much faster with the smaller P(OPh)₃ (cone angle θ = 128°) than for the more basic but larger PPh₃ (θ = 145°).[11] Similarly, the reactivity order observed for (Ind)Mo(CO)₃Br was PBu₃ > P(OMe)₃ > PPh₃ > P(OPh)₃.[2] It is unlikely that this steric argument can account for the difference in the ease of the associative pathway between (Ind)Mo(CO)₃X and 1 as the average metal-to-carbon bond distances are virtually identical.

Electronic effects are known to strongly influence the rates of associative substitution. For example, Rerek and Basolo observed that substitution by PPh₃ in the electron-deficient (η^5-C₅H₄NO₃)Rh(CO)₂ is 10⁴ times faster than in (η^5-C₅H₅)Rh-(CO)₂.[1a] Conversely, we observe that both associative substitution

and dissociative substitution are much slower in the anion (Ind)W(CO)₃⁻ than in neutral (Ind)W(CO)₃Cl. On the other hand, the infrared spectra of (Ind)Mo(CO)₃Cl and 1 differ only slightly and oppositely to their observed difference in reactivity.[12] Similar, spectroscopic measures of the electron density at the metal center differ only slightly for η^5-indenyl and η^5-cyclopentadienyl complexes. Ground-state electronic-effects do not account for the indenyl effect.

If significant steric and electronic differences between indenyl and cyclopentadienyl complexes do not exist and similar differences do not exist between (Ind)Mo(CO)₃Cl and 1, then what can account for the extraordinary effect of indenyl ligands on the rates of substitution? In the absence of ground-state effects, this phenomenon must be associated with the ability of the indenyl ligand to accommodate changes in electron density and bonding in the transition state for substitution. In our work and that of Mawby,[4] it is established that the indenyl effect can strongly influence both dissociative and associative substutution pathways. Yet, the oft-cited ring-slippage mechanisn can at best aid an associative pathway. It is more likely that both the greater polarizability of the π-electrons of the arene system and the ability of the indenyl ligand to distort structurally contribute to the unique ability of this ligand to facilitate diverse reaction pathways.

(12) The IR absorptions reported for (Ind)Mo(CO)₃Cl at 2063, 1995, and 1963 cm⁻¹ in CHCl₃²ᵈ are at higher energy than those for **1**. Thus substitution in the Mo complex should be faster, contrary to observation.

Contribution from the Laboratoire de Chimie Moléculaire, Unité Associée au CNRS, Parc Valrose, 06034 Nice, France

N-Protonations and N-Alkylation of Cyclenphosphorane. Synthesis and Crystal Structure of a Stable Phosphorus Compound with Two N-Protonated P–N Bonds

Frédéric Bouvier, Jean-Marc Dupart, and Jean G. Riess*

We recently reported that cyclenphosphorane (1) reacts with diborane to afford cyclenphosphorane–bis(borane) (2), revealing the unexpectedly strong basicity of the P-bonded apical nitrogen atoms in the polycyclic structure.[1]
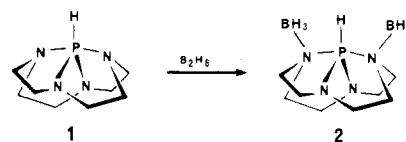
The isolation of **2** raised the following questions: What will be the direct action of a protic acid on **1** (P–N bond cleavage, alteration of the tetracyclic structure)? If not, how many nitrogen atoms can one protonate on **1**? Can the equatorial nitrogen atoms be protonated?

(9) Faller, J. W.; Crabtree, R. H.; Habib, A. *Organometallics* **1985**, *4*, 929–935.

(10) Mawby, A.; Pringle, G. E., *J. Inorg. Nucl. Chem.* **1972**, *34*, 525–530.

(11) Tolman, C. A. *Chem. Rev.* **1977**, *77*, 313–348.

(1) (a) Dupart, J.-M.; Le Borgne, G.; Pace, S.; Riess, J. G. *J. Am. Chem. Soc.* **1985**, *107*, 1202. (b) Dupart, J.-M.; Pace, S.; Riess, J. G. *J. Am. Chem. Soc.* **1983**, *105*, 1051. (c) Dupart, J.-M.; Grand, A.; Pace, S.; Riess, J. G. *Inorg. Chem.* **1984**, *23*, 3777. (d) Dupart, J.-M.; Grand, A.; Riess, J. G. *J. Am. Chem. Soc.* **1986**, *108*, 1168.

Under the action of hydracids, the P–N bond is generally readily cleaved to give the corresponding halophosphorus derivatives and ammonium halides; coordination of the phosphorus to a transition metal usually does not change this reactivity.[2] However, a few examples of compounds are known in which a P–N bond is not affected by hydracids: Harger and co-workers isolated some stable hydrochlorides of alkylphenylphosphinic amides RPhP(O)NH$_2$ but were unable to decide on the location of the proton.[3,4] Two more examples may be cited: a constrained bicyclic aminophosphine P-coordinated to a metal, which led under the action of gaseous HCl to the isolable and stable phosphorus–ammonium salt **3**,[2] and the ionic product **4**,[5] which results from the abstraction of the proton from HWCp(CO)$_3$ by **1**.

3

4
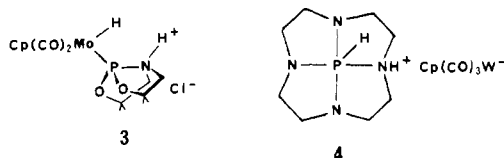
Finally, compound **5** was recently isolated; it exhibits one protonated P-bound apical nitrogen atom while the other is alkylated by a rhodium-borne CH$_2$ group.[6]
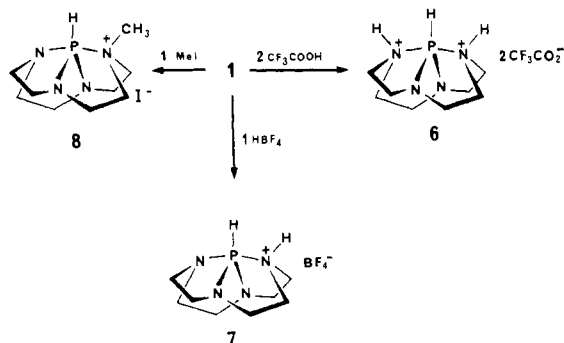
5
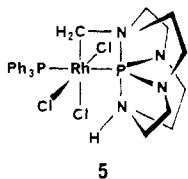
We were thus interested in the behavior of **1** toward protic acids or methyl iodide, which reactions are reported here.

Results and Discussion

Synthesis and Solution Data. Cyclenphosphorane[7] (**1**) reacts readily with 2 equiv of CF$_3$COOH to give the dication **6** in nearly quantitative yield (Scheme I). No evidence was found for any destruction of the polycyclic structure.

In solution, the ^{31}P NMR spectrum of **6** in CH$_3$CN exhibits a single sharp high-field doublet at −48 ppm characteristic of five-connected phosphorus with $^1J_{PH}$ = 780 Hz. The ^{13}C NMR spectrum displays only two CH$_2$ signals of equal intensity at 42.7 and 44.5 ppm; this can only be consistent with the presence of two protons on two nitrogen atoms symmetrically located in the

Scheme I

8

7

Figure 1. ORTEP drawing of 6.

Figure 2. Packing of molecules in the unit cell.

macrocycle. No exchange process appears to occur in the dication (from ^{13}C NMR data collected at variable temperature). No further protonation was achieved when an excess of the acid was added to **6**.

We also prepared the monocationic compound **7**, which is similar to that obtained by Lattman and co-workers through another route,[5] of which **4** is one example. The spectroscopic data of the two compounds are in good agreement. Trifluoroacetic and tetrafluoroboric acids were selected as proton sources because of the low nucleophilicity of CF$_3$COO$^-$ and BF$_4^-$ and the better solubility of the ionic products in common organic solvents. The dication with CF$_3$COO$^-$ as counteranions crystallized more readily than that with BF$_4^-$ while the reverse was found for the monocation.[8]

The action of 1 equiv of MeI on **1** yielded the phosphorane–ammonium salt **8** nearly quantitatively, thus establishing the nucleophilic character of the apical nitrogen in the polycyclic compound. The formulation of **8** was confirmed by elemental analysis and mass spectrometry. Its ^{1}H NMR spectrum exhibits a doublet at 2.65 ppm corresponding to the methyl group on the nitrogen atom with $^3J_{HP}$ = 10 Hz whereas the ^{31}P{^{1}H} NMR spectrum shows a single peak at −21 ppm in the pentacoordinated phosphorus region. Excess MeI did not lead to further alkylation under the experimental conditions chosen.

(2) Febvay, J.; Casabianca, F.; Riess, J. G. *J. Am. Chem. Soc.* **1984**, *106*, 7986 and references therein.
(3) Harger, M. J. P. *J. Chem. Soc., Perkin Trans. 1* **1975**, 514.
(4) Wong-Ng, W.; Nyburg, S. C.; Modro, T. A. *J. Chem. Soc., Chem. Commun.* **1980**, 195. Modro, T. A. *J. Chem. Soc., Chem. Commun.* **1980**, 201.
(5) Lattman, M.; Chopra, S. K.; Cowley, A. H.; Arif, A. M. *Organometallics* **1986**, *5*, 677.
(6) Burns, E. G.; Chu, S. S. C.; de Meester, P.; Lattman, M. *Organometallics* **1986**, *5*, 2383.
(7) Richman, J. E.; Atkins, T. J. *Tetrahedron Lett.* **1978**, 4333. Atkins, T. J.; Richman, J. E. *Tetrahedron Lett.* **1978**, 5149.
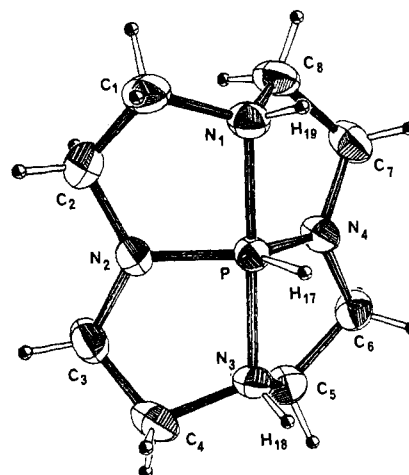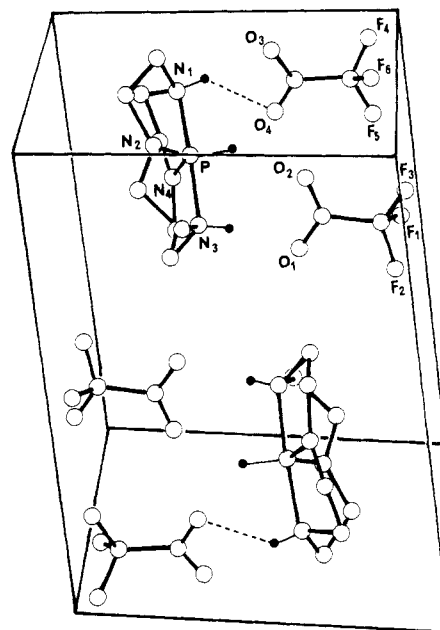
(8) Holmes, R. R.; Deiters, J. A. *J. Am. Chem. Soc.* **1977**, *99*, 3318.

Table I. Crystal Data for **6**

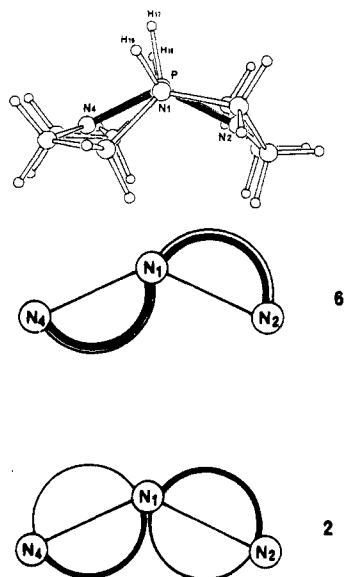|	
empirical formula	$C_{12}H_{19}N_4O_4F_6P$
fw	428.3
space group	$P\bar{1}$
a, Å	9.600 (3)
b, Å	11.603 (4)
c, Å	8.505 (3)
α, deg	109.2 (1)
β, deg	99.9 (1)
γ, deg	84.4 (1)
Z	2
d_{calcd}, g cm^{-3}	1.62
cryst dimens, mm	0.4 × 0.3 × 0.5
temp, °C	20
radiation	Mo Kα (0.710 69 Å)
monochromator	graphite
abs coeff, cm^{-1}	2.36
diffractometer	Enraf-Nonius CAD4
scan method	θ–2θ
hkl limits	0 to +11, −13 to +13, −10 to +10
2θ range, deg	2–50
scan width, deg	0.9 + 0.35 tan θ
programs used	Enraf-Nonius SDP
data collected	2930
data with $I > 3.0\sigma(I)$	2265
no. of variables	244
R	0.067
R_w	0.102
goodness of fit	3.89

Figure 3. ORTEP drawing of **6** along the N1–P–N3 axis and schematic views of **6** and **2** along this axis showing an "8" pattern for **2** and an "S" pattern for **6**.

Crystal Structure. An ORTEP plot of the dication and a plot of the packing of the molecules in the unit cell are shown in Figures 1 and 2, respectively. Selected bond lengths and bond angles are listed in Table II and the atomic positional parameters in Table III.

Structure **6** provides the first example of a bipyramidally surrounded phosphorus atom having two protonated apical nitrogens.

The equatorial hydrogen atom on phosphorus is well-located, and the arrangement of the five substituents around phosphorus is very close to the ideal trigonal-bipyramidal geometry.[9] The three equatorial atoms are coplanar to the phosphorus atom as shown by the sum of the equatorial angles about P (360°). It is interesting to note that the N2–P–N4 angle (127.2 (2)°) and the N2–P–H17 angle (125.7 (1)°) are rather large, whereas the third equatorial angle N4–P–H17 is strangely small (107.0 (1)°).

(9) Weast, R. C., Ed. *Handbook of Chemistry and Physics*, 60th ed.; CRC: Boca Raton, FL, 1979; p D-194.

Table II. Selected Bond Distances (Å) and Angles (deg) for **6**

P–N1	1.867 (4)	C7–C8	1.519 (6)
P–N3	1.864 (4)	C1–C2	1.496 (7)
P–N2	1.646 (3)	C3–C4	1.507 (6)
P–N4	1.629 (3)	C5–C6	1.507 (6)
P–H17	1.207 (1)	C9–O1	1.245 (5)
N3–H18	0.858 (3)	C9–O2	1.199 (5)
N1–H19	0.906 (3)	C9–C10	1.517 (7)
		C10–F1	1.304 (7)
N2–C2	1.461 (6)	C10–F2	1.254 (9)
N2–C3	1.445 (6)	C10–F3	1.266 (7)
N4–C7	1.440 (6)		
N4–C6	1.460 (5)	C11–O3	1.238 (5)
N1–C1	1.482 (4)	C11–O4	1.208 (6)
N1–C8	1.494 (6)	C11–C12	1.514 (7)
N3–C4	1.492 (5)	C12–F4	1.268 (8)
N3–C5	1.486 (5)	C12–F5	1.252 (6)
		C12–F6	1.311 (8)
N1–P–N3	175.7 (2)	N1–C1–C2	105.9 (3)
N2–P–N4	127.2 (2)	C1–C2–N2	105.5 (4)
N1–P–N2	89.1 (2)	N2–C3–C4	105.2 (3)
N1–P–N4	88.9 (2)	C3–C4–N3	105.7 (4)
N3–P–N2	89.0 (2)	N3–C5–C6	105.4 (3)
N3–P–N4	89.1 (2)	C5–C6–N4	105.1 (3)
N1–P–H17	95.6 (1)	N4–C7–C8	104.8 (3)
N3–P–H17	88.6 (1)	C7–C8–N1	104.6 (4)
N2–P–H17	125.7 (1)		
N4–P–H17	107.0 (1)	O3–C11–O4	126.7 (5)
		O3–C11–C12	117.1 (4)
P–N1–C1	108.1 (3)	O4–C11–C12	116.2 (4)
C1–N1–C8	114.5 (3)	C11–C12–F4	113.9 (5)
C8–N1–P	107.2 (3)	C11–C12–F5	116.4 (4)
H19–N1–C8	99.5 (3)	C11–C12–F6	111.4 (5)
H19–N1–P	103.1 (3)	F4–C12–F5	107.1 (5)
H19–N1–C1	123.0 (3)	F5–C12–F6	105.9 (7)
P–N2–C2	117.7 (3)	F6–C12–F4	100.7 (5)
P–N2–C3	118.4 (3)		
C2–N2–C3	120.6 (3)	O2–C9–O1	129.1 (4)
P–N3–C5	108.3 (3)	O2–C9–C10	116.6 (4)
P–N3–C4	108.1 (3)	O1–C9–C10	114.2 (4)
C5–N3–C4	115.1 (3)	C9–C10–F1	111.4 (5)
H18–N3–P	118.9 (3)	C9–C10–F2	114.3 (5)
H18–N3–C5	104.8 (3)	C9–C10–F3	115.7 (4)
H18–N3–C4	101.9 (4)	F1–C10–F2	104.8 (5)
P–N4–C6	118.8 (3)	F2–C10–F3	107.6 (6)
P–N4–C7	119.4 (3)	F3–C10–F1	101.6 (5)
C6–N4–C7	121.3 (3)		

P, N1, N3, and H17 and also coplanar. With respect to this latter plane, atoms H18 and H19 are located on the same side at significantly nonequal distances, 0.07 and 0.34 Å, respectively (Figure 3). These differences appear to be the consequence of hydrogen bonding between H19 and an oxygen atom of one of the CF_3COO^- counteranions (Figure 2). The intermolecular H19–O4 distance of 2.458 (4) Å is indeed shorter than the van der Waals approach (a van der Waals radius of 1.2 Å for H and 1.4 Å for O are generally accepted[10]) and indicates a bent hydrogen bond (angle N–H19–O4 = 147.3 (2)°). The other intermolecular H–O distances are all larger than 2.6 Å.

The equatorial P–N bonds are very short (1.646 (3) and 1.629 (4) Å) and the apical ones much larger (1.867 (4) and 1.864 (4) Å). These data are similar to those found for **2**.[1] As in the latter case, no π-contribution can be envisaged between phosphorus and the protonated nitrogens; hence, the bond distance of 1.87 Å, already found in **2**, can actually be considered as typical for an apical single bond between a bipyramidal phosphorus atom and a tetrahedral nitrogen atom. By contrast maximum $P_d\pi$–$N_p\pi$ bonding is achieved in the equatorial plane (the sums of the angles around N2 and N4 are 356.7 ± 2.7 and 359.5 ± 2.7°, respectively); this model is also in agreement with the observed absence of basicity (no protonation in the presence of an excess of hydracid).

(10) The monoprotonated product can be obtained with CF_3COOH whereas double protonation occurs with HFB_4.

Table III. Fractional Coordinates and Isotropic Thermal Parameters for **6**

atom	10^4x	10^4y	10^4z	$10B_{iso}$, Å^2
P	3937 (1)	2377.5 (8)	7027 (1)	20.5 (2)
N1	3692 (4)	1162 (3)	7935 (4)	27.0 (7)
N2	3178 (4)	1516 (3)	5178 (4)	27.7 (7)
N3	4033 (3)	3606 (3)	6090 (4)	23.6 (6)
N4	3161 (4)	3361 (3)	8506 (4)	25.1 (7)
C1	3378 (5)	18 (4)	6523 (5)	34.4 (9)
C2	2547 (5)	399 (4)	5105 (6)	36 (1)
C3	2752 (5)	2060 (4)	3858 (5)	35 (1)
C4	3772 (5)	3056 (4)	4220 (5)	34.1 (9)
C5	3027 (4)	4624 (3)	6806 (5)	28.6 (8)
C6	3036 (4)	4643 (3)	8588 (5)	28.1 (9)
C7	2779 (5)	2979 (4)	9817 (5)	32.8 (9)
C8	2553 (5)	1620 (4)	9012 (5)	33.0 (9)
C9	2509 (5)	−3487 (4)	13562 (5)	30.8 (9)
C10	948 (5)	−3746 (5)	13228 (7)	45 (1)
O1	3300 (3)	−4410 (3)	13087 (5)	42.2 (8)
O2	2810 (4)	−2437 (3)	14196 (6)	64 (1)
F1	473 (5)	−4125 (6)	11619 (6)	109 (2)
F2	655 (4)	−4566 (4)	13764 (7)	152 (1)
F3	121 (4)	−2830 (5)	13747 (7)	111 (2)
C11	3142 (5)	8322 (4)	−259 (6)	37 (1)
C12	1551 (6)	8231 (5)	−712 (8)	50 (1)
O3	3593 (4)	9314 (3)	698 (5)	49.6 (9)
O4	3840 (5)	7416 (4)	−888 (7)	81 (1)
F4	966 (4)	8917 (4)	−1580 (6)	95 (1)
F5	1103 (5)	7182 (4)	−1460 (10)	138 (2)
F6	924 (5)	8669 (7)	630 (6)	141 (2)

The P–H17 bond lengths are similar in **6** and **2** and very short as expected in the equatorial plane of a trigonal bipyramid.

Differences between the structures of **6** and **2** are observed when examining the conformations of the five-membered rings. A schematic view of **6** and **2** along the N1–P–N3 axis (Figure 3) shows an "8" pattern for **2** and an "S" pattern for **6** (note in the latter case the eclipsed positions of the cycles in the foreground and background of the equatorial plane containing atoms P, N4, N2, and H17).

Experimental Section

Instrumentation. NMR spectra were obtained on a Bruker WH-90 spectrometer (chemical shifts are given in ppm downfield from external Me$_4$Si for ^{13}C, from external 85% H$_3$PO$_4$ for ^{31}P, and from internal CCl$_3$F for ^{19}F). Infrared spectra were recorded on a Bruker IFS 45 spectrophotometer. Mass spectra were obtained on a R 10 Ribermag L 10 instrument. Molar conductances were determined with a Tacussel CD6NG electronic conductometer.

Synthesis of Cyclenphosphorane–Bis(trifluoroacetic acid) (6). A 0.123-mL portion (1.66 mmol, Aldrich) of trifluoroacetic acid was added to a solution of 0.162 g (0.81 mmol) of cyclenphosphorane (**1**)^7 in 5 mL of CH$_2$Cl$_2$ at −40 °C. A white precipitate was formed immediately. It was filtered and washed repeatedly with CH$_2$Cl$_2$, yielding 0.309 g (90%) of a white hygroscopic powder soluble in CH$_3$CN. Anal. Calcd for C$_{12}$H$_{19}$N$_4$O$_4$F$_6$P: C, 33.67; H, 4.47; N, 13.09; P, 7.24. Found: C, 33.73; H, 4.50; N, 13.17; P, 6.93. ^{1}H NMR (CD$_3$CN): δ 11.9 (0.5 H,^{11} H–P), 10.6 (2 H, H–N$^+$), 3.2 (m, 16.5 H). ^{31}P NMR (CH$_3$CN): δ −48.0 (d, $^1J_{PH}$ = 780 Hz). ^{13}C NMR (CD$_3$CN): δ +44.5 (d, $^2J_{CP}$ = 7 Hz), +42.7 (d, $^2J_{CP}$ = 13 Hz). IR (KBr pellet, cm^{-1}): ν(N–H) 2806 (w), ν(P–H) 2450 (w), ν(CO) 1678 (s).

Synthesis of Cyclenphosphorane–Tetrafluoroboric Acid (7). A solution of tetrafluoroboric acid (54%) (0.08 mL, 1.2 mmol, Fluka) in Et$_2$O was added to 0.24 g (1.2 mmol) of **1** in 5 mL of CH$_2$Cl$_2$ at −35 °C. The solution was allowed to warm to room temperature. Evaporation then led to a gummy product, which was taken up in 50 mL of Et$_2$O with stirring overnight. Filtration yielded 0.28 g (83%) of a white, slightly hygroscopic product, soluble in toluene, CH$_2$Cl$_2$, and CH$_3$CN. ^{1}H NMR (CD$_2$Cl$_2$): δ 11.4 (0.5 H,^{11} H–P), 6.7 (s, 1 H, H–N$^+$), 2.9 (m, 16.5 H). ^{31}P NMR (CH$_3$CN): δ −47.7 (d, $^1J_{PH}$ = 700 Hz). ^{13}C NMR (CD$_3$CN): δ +44.2 (d, $^2J_{CP}$ = 8.8 Hz). ^{19}F NMR (CH$_2$Cl$_2$): δ −152 (s). IR (KBr pellet, cm^{-1}): ν(P–H) 2375 (w). Molar conductance (10^{-3} *m* in acetone): 116 Ω^{-1} cm^2 mol^{-1}.

(11) $^1J_{H–P}$ and δ$_{H–P}$ cannot be determined from the ^{1}H NMR spectrum because the upfield branch of the doublet is masked by the signals of the methylenes. Only the chemical shift of the downfield branch is given.

Synthesis of Cyclenphosphorane–Methyl Iodide (8). One molar equivalent of MeI (0.024 mL, 0.38 mmol, Aldrich) was added to a solution of **1** (0.077 g, 0.38 mmol) in 5 mL of CH$_2$Cl$_2$ with stirring at room temperature. The reaction mixture remained clear. Evaporation of the solvent led quantitatively to 0.131 g of a white hygroscopic powder. Anal. Calcd for C$_9$H$_{20}$N$_4$PI: C, 31.59; H, 5.89; N, 16.37; P, 9.05. Found: C, 31.20; H, 5.70; N, 16.40; P, 8.93. ^{1}H NMR (CDCl$_3$): δ 10.9 (0.5 H,^{11} H–P), 3.0 (m, 16.5 H), 2.65 (d, 3 H, $^3J_{HP}$ = 10 Hz). ^{31}P NMR (CH$_2$Cl$_2$): δ −21.2 (d, $^1J_{PH}$ = 740 Hz). ^{13}C NMR (CD$_2$Cl$_2$): δ 52.1, 51.7, 45.4, 45.2, 44.7, 43.8, 42.0, 41.7, 40.6, 40.3. IR (KBr pellet, cm^{-1}): ν(P–H) 2400 (w). MS (chemical ionization with NH$_3$, *m/e*): (M − I)H$^+$ (91%), (M − MeI)H$^+$ (100%).

Crystal Structure. Suitable colorless platelike crystals were obtained from a saturated solution of **6** in CH$_3$CN cooled to −30 °C. These crystals are triclinic and belong to space group P$\bar{1}$. The unit cell parameters given in Table I have been refined by least squares from angular positions of 25 reflections.

The intensities of 2930 reflections were collected with an Enraf-Nonius CAD4 automated diffractometer. A variation of 2.1% in the intensity of the standard reflections recorded periodically was observed during the data collection. The data were corrected for Lorentz and polarization factors but not for absorption. The atomic scattering factors were taken from Cromer and Waber.^{12} The structure was solved by direct methods (MULTAN).^{13} Fourier synthesis allowed the location of all non-hydrogen atoms. All programs used were from the SDP program library.^{14} The hydrogen atoms were located from difference Fourier synthesis or were placed in calculated positions on their parent carbons (C–H = 0.96 Å). They were introduced isotropically but not refined (B = 5 Å^2). Convergence of the full-matrix least-squares refinement gave residuals R = 0.067 and R_w = 0.102. In all refinements the function minimized was $\sum w(|F_o| - |F_c|)^2$, where $w = 1/\sigma^2(F)$.

Acknowledgment. We wish to thank Dr. M. Pierrot from the University of Aix-Marseille for performing the X-ray study.

Registry No. **1**, 64317-97-1; **6**, 112067-96-6; **7**, 112067-97-7; **8**, 112021-59-7.

Supplementary Material Available: Positional parameters of hydrogen atoms (Table A) and thermal parameters (Table B) (2 pages); a table of observed and calculated structure factors (8 pages). Ordering information is given on any current masthead page.

(12) Cromer, D. T.; Waber, J. T. *Acta Crystallogr.* **1965**, *18*, 104. Cromer, D. T. *Acta Crystallogr.* **1965**, *18*, 17.

(13) Main, P.; Fiske, S. J.; Hall, S. E.; Lessinger, L.; Germain, G.; Declercq, J. P.; Woolfson, M. M. *Multan 80. A System of Computer Programs for Automatic Solution of Crystal Structures from X-ray Diffraction Data*; University of York, York, England, and University of Louvain, Louvain, Belgium, 1980.

(14) Frenz, B. A. In *Computing in Crystallography*; Schenk, H., Olthof-Hazekamp, R., van Koningsveld, H., Bassi, G. C., Eds.; Delft University Press: Delft, The Netherlands, 1978; pp 44–71.

Contribution from the Department of Physical Sciences, Trent Polytechnic, Clifton Lane, Nottingham NG11 8NS, U.K.

Reply to "Extended Hückel Calculations and the Role of d Orbitals in Transition-Metal-Cluster Bonding"[1]

R. G. Woolley

In a recent note^1 in this journal, D. G. Evans gave a detailed presentation of some extended Hückel (EH) calculations on Fe$_5$ cluster species and used his results to comment on two earlier papers on mine^{2,3} devoted to the bonding in transition-metal-cluster compounds. There is now general agreement about the importance of the metal d electrons in transition-metal-cluster

(1) Evans, D. G. *Inorg. Chem.* **1986**, *25*, 4602.
(2) Woolley, R. G. *Inorg. Chem.* **1985**, *24*, 3519.
(3) Woolley, R. G. *Inorg. Chem.* **1985**, *24*, 3525.